A. Brömme, C. Busch, N. Damer, A. Dantcheva, M. Gomez-Barrero, K. Raja,
C. Rathgeb, A. Sequeira, and A. Uhl (Eds.): BIOSIG 2021,
Lecture Notes in Informatics (LNI), Gesellschaft für Informatik, Bonn 2021

Assessment of Sensor Ageing-Impact in Air Travelled Fingerprint Capturing Devices

Christof Kauba[1], Simon Kirchgasser[1], Robert Jöchl[1], Andreas Uhl[1]

Abstract: Biometric recognition performance is affected by many factors, like varying acquisition conditions or ageing related effects, commonly denoted as biometric template ageing. Image sensor ageing, being part of biometric template ageing and a sub-field of image and video forensics, leads to defective pixels due to cosmic radiation, depending on the altitude. So far, image sensor ageing has only been a peripheral target in fingerprint research. We investigate the impact of image sensor ageing on various fingerprint capturing devices, including optical, capacitive and thermal ones. We established a fingerprint ageing dataset utilising 10 capturing devices which travelled on an air-plane for 127 days (to increase the number of developed defects). By evaluating the samples captured prior to their travel and afterwards using several state-of-the-art fingerprint quality metrics as well as minutiae-based fingerprint recognition systems we quantify the effect of image sensor ageing on fingerprint recognition. Furthermore, by employing a defect detection technique we quantify the number of defects developed during that period.

Keywords: Fingerprint Recognition, Biometric Template Ageing, Fingerprint Sensor Ageing, Performance Evaluation, Quality Evaluation.

1 Introduction

Fingerprints (FP) are one of the most frequently used biometric modalities for authenticating people in many devices and applications in everyday life, e.g. in smartphones, laptops or border control. Fingerprint recognition systems are also deployed for long-term usage, e.g. for passports typically having a validity period of 10 years, during which time the biometric data (FP and face) is not updated and should be robust against ageing effects, which are referred to as "biometric template ageing". According to the ISO/IEC 19795-1:2006 standard [IS06] these include biological subject ageing, changes in subject's behaviour, changes in the acquisition conditions and ageing of the capturing device itself.
Many biometric capturing devices, especially optical FP sensors, contain an optical image sensor, which develops in-field defects in the form of isolated defective pixels over time. These defective pixels exhibit different characteristics than at manufacturing time and appear as point like, spiky shot noise in an output image. There is extensive literature about image sensor ageing related defects and the source causing these defects [Th07, Th08, Ch13, Du07, Le10, Le09, Le08]. In-field sensor defects are permanent, the number of defects increases linearly with time and inter-defect times follow an exponential distribution, indicating a constant defect rate, are randomly distributed over the sensor area, with no significant bias towards short or long distances, i.e. no defect clustering. Evaluation on various types of cameras over several years indicate that cosmic radiation, actually the neutrons of the cosmic rays are most likely causing these single pixel defects.

[1] Department of Computer Sciences, University of Salzburg, AUSTRIA, {ckauba, skirch, rjoechl, uhl}@cs.sbg.ac.at

The question if and how image sensor ageing affects the performance of the whole biometric system is still ongoing research. Bergmller et al. [Be14] showed that the sensor ageing related pixel defects may have an influence on iris recognition. Kauba et al. did some work on finger veins [KU15b], hand veins [KU15a] and fingerprints [KU16] where they concluded that image sensor ageing is negligible in practical applications. However, they only simulated the in-field sensor defects rather than letting real devices "age".
The focus of this work is on the effect of image sensor ageing in practical applications of FP recognition systems and thus, to find out which role it plays within the scope of biometric template ageing. In order to evaluate the impact of in-field sensor defects on fingerprint recognition, a FP ageing dataset using 10 different commercial-off-the-shelf FP capturing devices, including optical, capacitive and thermal ones, divided into two sessions, was established. The first session is the reference session. As the total flux of radiation depends on the altitude, which is about 300-400 times higher at 30,000 feet than on ground level, the capturing devices have been situated on board of a long-haul plane for 127 days to expose them to a higher cosmic ray radiation total flux. Afterwards the second capturing session with the same subjects was conducted. By comparing the samples of both sessions using 1) several FP quality metrics and 2) minutiae-based FP recognition systems, the impact of image sensor ageing induced single pixel defects on the biometric recognition performance can be quantified.
The rest of this work is organised as follows: Section 2 explains the experimental set-up, including details about the FP ageing dataset, the utilised FP capturing devices, the FP quality metrics, the FP recognition systems and the defect detection algorithm. The empirical analysis results are presented in Section 3 and Section 4 concludes this paper.

2 Experimental Set-up

The key aspect of the experimental analysis in order to quantify the effects introduced by FP sensor ageing is that the acquired FP samples were captured before (2 sessions named 'before' and 'reference') and after (1 session named 'after') the utilised capturing devices have been exposed to a higher flux level of cosmic radiation.

2.1 Dataset

As mentioned in Section 1, most studies on image sensor ageing done so far observed corresponding effects after experimentally simulating the ageing process. Naturally, the increase of sensor defects causing detectable sensor ageing effects are introduced by cosmic radiation, which is depending on the altitude. To induce an accelerated ageing process, the capturing devices were exposed to a higher amount of cosmic ray total flux by situating them on a Boeing 777-200 long-haul air plane (the flux in 30,000 feet is about 300-400 times higher than at ground level) for about 127 days while it was travelling around the world. This corresponds to a sensor "age" of about 100 years after the travel (350 times the flux on ground level * 85% of the time at cruise altitude * 127 days / 365 days = 102.85 years). Figure 1 shows the box with the capturing devices and the location on the plane and an excerpt of the flight protocol.

Fig. 1: FP capturing devices situated on the plane: top left - location on the place, bottom left - flight protocol excerpt, top right - capturing devices stored in the aluminium box, bottom right - aluminium box top side.

10 different commercial off-the-shelf FP capturing devices, the optical Lumidigm V311, Lumidigm M311, DigitalPersona URU5160, Suprema RealScan G1, the capacitive Integrated Biometrics Columbo, Integrated Biometrics Curve, Zvetco Verifi P5000, DigitalPersona Eikon 710 Touch, Upek Eikon II Swipe and the thermal one Next Biometrics NB-3010-U were used to acquire the FP samples. In the following they are abbreviated as V311, M311, URU5160, G1, IBCol., IBCur., P5000, Touch, Swipe and NB-U, respectively. None of those devices has an electromagnetic shielding and they have not been stored in an isolated storage but inside an aluminium case. The 'before' and 'after' session contain FP samples from 59 subjects. All 10 fingers of each subject were acquired, 5 images per finger, which results in about 2800 samples for each capturing device per session in total. All samples exhibit an image resolution of 500 dpi and have been captured under the same environmental conditions to reduce other influencing factors to a minimum. These samples are a subset of a publicly available database and can be obtained from `http://wavelab.at/sources/PLUS-MSL-FP/`. The remaining third session, 'reference', has been captured before mounting the devices on the air plane similar like the session 'before'. Opposed to the other two sessions the aim was not to capture as much FP specific information, instead the focus was on capturing samples that contain as less FP structure as possible which was achieved by positional variations of the finger in order to capture as much as possible background information (see Figure 2). The uniform background helps to detect possible sensor defects (hot and stuck pixel) which are likely to be

overlaid by the presence of FP information. In total this 'reference' subset contains 8000 FP samples acquired from 2 subjects using their right index and middle finger. For each finger 200 samples were captured which results in 400 images per subject.

Fig. 2: FP samples contained in the dataset: first two - samples from 'before', 3rd and 4th - samples from 'reference' and 5th and 6h - samples from 'after'. Examples were acquired with IBColumbo.

2.2 Quality Measures, Recognition Systems and Defect Detection Algorithm

A three step analysis was performed to measure the impact on the biometric performance. At first, the possible impact on the FP samples' quality is evaluated by applying several FP quality metrics including the current state-of-the-art metric NIST FP Image Quality 2.0 (NFIQ 2.0 - `https://github.com/usnistgov/NFIQ2`) as well as eleven quality metrics proposed by [OŠB16], namely frequency domain analysis (FDA), Gabor quality (GAB), Gabor-Shen quality (GSH), local clarity score (LCS), orientation flow (OFL), orientation certainty level (OCL), ridge-valley uniformity (RVU) and radial power spectrum (RPS).
Second, the impact on the recognition performance is quantified in terms of the equal error rate (EER) by calculating 5,920 mated and 4,335,000 non-mated comparison scores for each capturing device and evaluated session, by employing two fingerprint systems: ANSI & ISO SDK developed by Innovatrics (`https://www.innovatrics.com`) and VeriFinger SDK 11.0 developed by Neurotechnology (`https://www.neurotechnology.com`).
Finally, the developed in-field sensor defects are detected and quantified. In principle, in-field sensor defects can be localised with the help of calibration images (e.g. flat-field images). However, the acquisition of such calibration images is hardly possible with FP sensors (most of them only capture an image if they detect a finger on the sensor). Thus, the presence of in-field sensor defects must be determined from regular FP images. A simple approach to threshold the median filter residual variance, as suggested in [FG11] is utilised. A pixel is considered defective if $\sigma(\vec{r})^2 > t$, where $\vec{r}$ is a vector containing the median filter residual values of an arbitrary but fixed pixel over the set of images used for detection, t is a threshold defined by the average residual variance of all pixels plus the standard deviation times an adaptive weight w. The median filter is able to filter out a single point defect in the middle of a homogeneous image region, but it responds on structured image regions (like the ridges and valleys in FP images) as well. This raises the question of how reliable the defect detection method works with FP images.
To evaluate the reliability of the defect detection algorithm, synthetically created defects are embedded into the available FP images from the 'after' session using a sensor ageing simulation algorithm [KU16, Be14]. At first a defect map with uniformly distributed defects based on the defined parameters is created and then applied to the output images. The parameters are estimated based on the empirical formula proposed in [Ch13] as done

in [KU16]. The resulting rate of 0.244 defects / (MP * year) was multiplied by 400 (due to the higher cosmic ray total flux at 30,000 feet) and $\mu = 0.15$ (exponential distribution) was adopted for this work (correct parameter settings are less relevant for evaluating the defect detection performance). The resulting defect maps are used as ground-truth and the precision $= \frac{TP}{TP+FP}$ is evaluated for the detection method parameter w. TP (True Positives) denotes the correctly detected embedded defects and FP (False Positives) represents additional defect candidates.

3 Experimental Results

In the following we present the quality and performance evaluation results as well as the sensor defect detection results together with a results discussion.

3.1 Quality Evaluation

	quality	NFIQ 2.0	FDA	GAB	GSH	LCS	OFL	OCL	RVU	RPS
before	mean	46.22	0.45	643.94	563.55	0.62	0.62	0.59	751.14	901.25
	median	50.00	0.45	668.39	699.50	0.62	0.63	0.51	672.50	689.06
	std	22.31	0.05	163.78	154.67	0.18	0.17	0.18	174.61	213.71
after	mean	46.00	0.45	649.28	568.22	0.61	0.61	0.58	757.38	908.72
	median	50.00	0.45	665.05	692.63	0.61	0.62	0.50	672.49	684.42
	std	22.65	0.05	165.11	155.93	0.17	0.16	0.18	176.03	226.49

Tab. 1: Mean, median and standard deviation (std) of quality metrics applied on the used FP samples.

The FP quality metrics evaluation results are presented in Table 1. The mean, median and std have been calculated over all quality values with no regard to a specific sensor type. Other results on this dataset showed that the quality depends on the capturing devices' choice and thus, sensor specific fluctuations are detectable. However, even if there are slight fluctuations between the two sessions (before and after), they are due to the used quality metric as all of them measure different characteristics of the FP. There are no consistent changes detectable in the FP quality. Hence, possibly existing sensor defects do not seem to have any influence on the quality of the FP samples in terms of FP quality.

3.2 Recognition Performance

The quality analysis of the FPs did not indicate an influence of the image sensor ageing. So the next step was to quantify the effect on the recognition performance. In Figure 3 the EER results of before and after session are presented. The trend is highly depending on the FP capturing device and similar for both recognition systems (with Verifinger achieving lower EERs than Innovatrics ANSI). For example using Touch and IBCol. an improved recognition performance can be reported for the 'after' session samples. VeriFinger's EER of 0.29% and 0.27% improved to 0.16% and 0.08%, respectively. On the other hand, for URU5160, IBCur. und NB-U, the EER for session 'after' is inferior to the 'before' case (before: 0.16%, 0.79% and after: 0.49%, 0.94% for Innovatrics ANSI). Once again, no

general deterioration in the EER is discernible and thus, no influence of potential sensor defects with regard to the recognition performance can be detected.

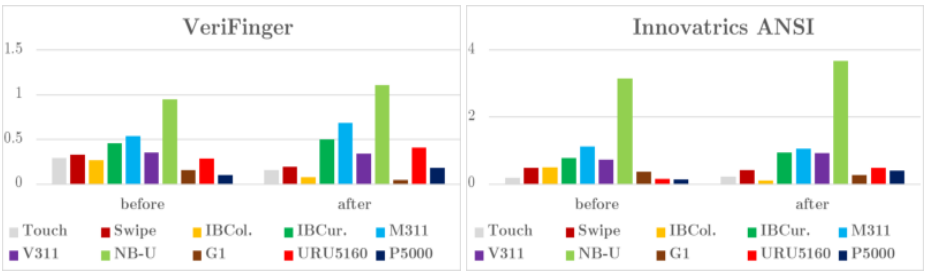

Fig. 3: Recognition performance - EER results in percent, left: VeriFinger, right: Innovatrics ANSI.

3.3 Defect Detection

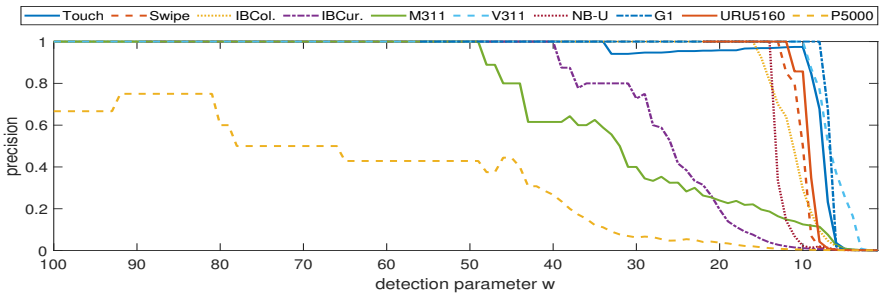

Fig. 4: Precision of the detected embedded defects over the detection parameter *w*.

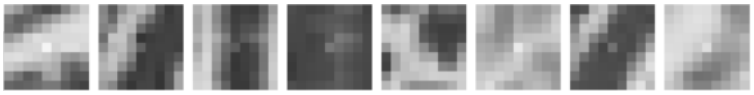

(a) detected synthetic embedded defect, offset = 0.12498

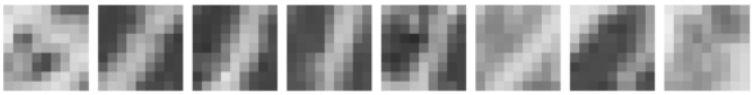

(b) detected non-embedded defect candidate

Fig. 5: Example for the visual inspection of the detected non-embedded defect candidates.

As neither the FP quality nor the recognition performance evaluation revealed any considerable performance degradations, the next step was to verify if there are any in-field sensor defects detectable at all. By analysing the 'after' session samples with the embedded defects, we can determine whether the detection method works with FP images and whether real defects are present in addition to the embedded defects. Figure 4 shows the precision of the detected embedded defects. As illustrated, all FP sensors (except the P5000) achieve a precision of 100% (i.e. only embedded defects are detected, $FP = 0$) for higher parameter values. This indicates that the used defect detection method can reliably detect point defects (such as the synthetic embedded ones), at least those with a high offset. In addition,

a precision of 100% indicates that there are very likely no real defects with an offset similar to that of the detected synthetic defects. To determine whether the candidates found in addition to the embedded defects are real defects, a visual inspection was performed. This is illustrated in Figure 5, where image patches extracted around a detected defect candidate are compared to image patches (extracted from the same images) of a detected embedded defect. Based on the visual inspection, we can assume that there are no detectable (strong) point defects (for any of the evaluated FP sensors) present in the 'after' session samples. However, if weak (with a small offset) defects are present, they will not affect the FP quality or FP recognition performance. The complete absence of (strong) defects indicates that the evaluated FP sensors either do not develop any in-field defects or they are able to suppress these single pixel defects (e.g. by applying image processing techniques).

4 Conclusion

In order to analyse the potential impact of image sensor ageing on FP recognition systems in general and on FP capturing devices in particular, a FP ageing dataset using 10 different FP capturing devices, including optical, capacitive and thermal ones was established. The capturing devices were situated on an air plane for 127 days to expose them to a higher cosmic radiation flux. The samples acquired in the sessions before and after situating the devices on the plane were evaluated using several FP image quality metrics and two minutiae-based FP recognition systems. In addition, an image sensor defect detection technique was utilised to quantify the number of developed defects.
The results of the FP quality assessment and the FP recognition performance suggest that even the increased level of cosmic ray radiation flux had no impact on the FP samples, neither in terms of the FP quality nor in terms of the biometric recognition performance. Moreover, the applied defect detection did not even result in a single detectable defect in all of the FP capturing devices.
Hence, the FP capturing devices either do not develop any defects at all or they employ some kind of defect concealment (during image post-processing done by the capturing device itself). Hence, there is no influence on the biometric quality and recognition performance which confirms the synthetic evaluation results of Kauba et. al [KU16] that in practice image sensor ageing is not a problem for FP recognition. Thus, these FP devices can be employed as an access control system for the cockpit door on an aircraft.
Due to the limited space the study presented only a first insight. The future work will include a more detailed per sensor analysis (quality as well as recognition performance), relating the results to the type of sensor (optical, capacitive, thermal) and analysing a potential correlation of the sensor ageing effects with the type of sensor. A further exposure to radiation with a dosimeter in parallel to measure the exact amount of radiation as well as an exposure to a controlled radiation (e.g. medical radiation device) are planned.

Acknowledgements

We gratefully thank the Austrian Airlines for their cooperation, situating the FP capturing devices on one of their air planes for 127 days in 2017. Furthermore, the current study received funding from the FFG KIRAS project BioCapture under grant No. 873462.

References

[Be14] Bergmüller, Thomas; Debiasi, Luca; Uhl, Andreas; Sun, Zhenan: Impact of sensor ageing on iris recognition. In: Proceedings of the IAPR/IEEE International Joint Conference on Biometrics (IJCB'14). 2014.

[Ch13] Chapman, Glenn H; Thomas, Rohit; Koren, Zahava; Koren, Israel: Empirical formula for rates of hot pixel defects based on pixel size, sensor area, and ISO. In: IS&T/SPIE Electronic Imaging. International Society for Optics and Photonics, p. 8 pages, 2013.

[Du07] Dudas, Jozsef; Wu, Linda M; Jung, Cory; Chapman, Glenn H; Koren, Zahava; Koren, Israel: Identification of in-field defect development in digital image sensors. In: Electronic Imaging 2007. International Society for Optics and Photonics, p. 8 pages, 2007.

[FG11] Fridrich, Jessica; Goljan, Miroslav: Determining approximate age of digital images using sensor defects. In (Memon, Nasir D.; Dittmann, Jana; Alattar, Adnan M.; III, Edward J. Delp, eds): Media Watermarking, Security, and Forensics III. volume 7880. International Society for Optics and Photonics, SPIE, pp. 49 – 59, 2011.

[IS06] ISO 19795-1:2006: Information technology–Biometric performance testing and reporting–Part 1: Principles and framework. Standard, International Organization for Standardization, 2006.

[KU15a] Kauba, Christof; Uhl, Andreas: Robustness Evaluation of Hand Vein Recognition Systems. In: Proceedings of the International Conference of the Biometrics Special Interest Group (BIOSIG'15). Darmstadt, Germany, p. 8, 2015.

[KU15b] Kauba, Christof; Uhl, Andreas: Sensor Ageing Impact on Finger-Vein Recognition. In: Proceedings of the 8th IAPR/IEEE International Conference on Biometrics (ICB'15). Phuket, Thailand, pp. 1–8, May 2015.

[KU16] Kauba, Christof; Uhl, Andreas: Fingerprint Recognition under the Influence of Sensor Ageing. IET Biometrics, 4(6):245–255, 2016.

[Le08] Leung, Jenny; Dudas, Jozsef; Chapman, Glenn H; Koren, Zahava; Koren, Israel: Characterization of pixel defect development during digital imager lifetime. In: Electronic Imaging 2008. International Society for Optics and Photonics, pp. 1–12, 2008.

[Le09] Leung, Jenny; Chapman, Glenn H; Koren, Zahava; Koren, Israel: Statistical identification and analysis of defect development in digital imagers. In: IS&T/SPIE Electronic Imaging. International Society for Optics and Photonics, pp. 1–12, 2009.

[Le10] Leung, Jenny; Chapman, Glenn H; Choi, Yong H; Thomas, Rohit; Koren, Zahava; Koren, Israel: Analyzing the Impact of ISO on Digital Imager Defects with an Automated Defect Trace Algorithm. In: Proc. SPIE. volume 7536, p. 8 pages, 2010.

[OŠB16] Olsen, Martin Aastrup; Šmida, Vladimír; Busch, Christoph: Finger image quality assessment features–definitions and evaluation. IET Biometrics, 5(2):47–64, 2016.

[Th07] Theuwissen, Albert JP: Influence of terrestrial cosmic rays on the reliability of CCD image sensors-Part 1: Experiments at room temperature. Electron Devices, IEEE Transactions on, 54(12):3260–3266, 2007.

[Th08] Theuwissen, Albert JP: Influence of Terrestrial Cosmic Rays on the Reliability of CCD Image Sensors-Part 2: Experiments at Elevated Temperature. Electron Devices, IEEE Transactions on, 55(9):2324–2328, 2008.